Global Analysis of Protein−Protein Interactions Reveals Multiple CYP2E1−Reductase Complexes[†]

Arvind P. Jamakhandi,[‡] Petr Kuzmic,[§] Daniel E. Sanders,[‡] and Grover P. Miller*,[‡]

Department of Biochemistry and Molecular Biology, University of Arkansas for Medical Sciences, Little Rock, Arkansas 72205, and BioKin, Ltd., Pullman, Washington 99163

ABSTRACT: Although a single binary functional complex between cytochrome P450 (P450 or CYP for a specific isoform) and cytochrome P450 reductase (CPR) has been generally accepted in the literature, this simple model failed to explain the experimentally observed catalytic activity of recombinant CYP2E1 in dependence on the total concentration of the added CPR-K56Q mutant. Our rejection of the simplest 1:1 binding model was based on two independent lines of experimental evidence. First, under the assumption of the 1:1 binding model, separate analyses of titration curves obtained while varying either P450 or CPR concentrations individually produced contradictory results. Second, an asymmetric Job plot suggested the existence of higher order molecular complexes. To identify the most probable complexation mechanism, we generated a comprehensive data set where the concentrations of both P450 and P450 were varied simultaneously, rather than one at a time. The resulting two-dimensional data were globally fit to 32 candidate mechanistic models, involving the formation of binary, ternary, and quaternary P450·CPR complexes, in the absence or presence or P450 and CPR homodimers. Of the 32 candidate models (mechanisms), two models were approximately equally successful in explaining our experimental data. The first plausible model involves the binary complex P450·CPR, the quaternary complex $(P450)_2 \cdot (CPR)_2$, and the homodimer $(P450)_2$. The second plausible model additionally involves a weakly bound ternary complex $(P450)_2 \cdot CPR$. Importantly, only the binary complex P450·CPR seems catalytically active in either of the two most probable mechanisms.

Protein−ligand and protein−protein interactions are fundamental to biological processes such as signal transduction, chemical transformations, and electron transport. An understanding of the role of these processes in biological function requires the identification of the detailed interaction mechanisms. These details provide a framework in which to understand how the process of molecular recognition maintains proper homeostasis or leads to deleterious conditions. In this study, we characterize the details of protein−protein interactions involving cytochrome P450 (P450)[1] and the cytochrome P450 reductase (CPR). Traditional experimental protocols and data-analytic methods applied to this two-component system failed to provide a clear answer regarding the binding stoichiometry. We describe an alternative data-analytic approach applicable to any multicomponent system. The method is based on a general numerical analysis of simultaneous biochemical equilibria, without any restriction on the number of component molecular species or the number of complexes they form (1). Our results indicate the involvement of the quaternary complex $(P450)_2 \cdot (CPR)_2$, in addition to possible involvement of the ternary complex $(P450)_2 \cdot CPR$, the ternary complex $P450 \cdot (CPR)_2$, or both ternary complexes.

Microsomal P450 enzymes are major catalysts in the oxidative transformation of a structurally diverse class of compounds including steroids, fatty acids, hormones, antibiotics, and a wide variety of artificially produced chemicals (xenobiotics), such as drugs, food additives, and environmental contaminants (2). P450s convert lipid-soluble molecules to more water-soluble forms and, in effect, modulate transport and other chemical properties. To accommodate a wide array of compounds, typical P450 enzymes have evolved low specificity and activity toward substrates, making interpreting and predicting their catalytic properties difficult. Localized to the endoplasmic reticulum, the membrane-bound P450 is best considered to be an aggregate of multiple distinct P450s associating with redox partners, the obligatory cytochrome P450 reductase (CPR) and in some cases cytochrome b_5 (cyt b_5) (reviewed in ref 3). The resulting protein−protein interactions ultimately define activity for P450s.

Understanding the biological impact of P450 activity requires knowledge of the identity of the P450 functional complex and the mechanism modulating its formation. Because the estimated molar ratio for P450 and CPR in membranes is approximately 20:1 (4) to 40:1 (5), one of the

---

* Corresponding author. Telephone: 501-526-6486. Fax: 501-686-8169. E-mail: millergroverp@uams.edu.

[‡] University of Arkansas for Medical Sciences.

[§] BioKin, Ltd.

[1] Abbreviations: P450, cytochrome P450; CYP, specific cytochrome P450 isoform; CPR, cytochrome P450 reductase; CPR-K56Q, cytochrome P450 reductase with Lys56Gln substitution; pNP, *p*-nitrophenol; pNC, *p*-nitrocatechol; $NADP^+$, nicotinamide adenine dinucleotide phosphate (oxidized); AIC_c, Akaike information criterion.

Scheme 1: Formation and Catalytic Activity of the Simplest (Binary) Functional Complex between P450 and CPR[a]

$$P + R \underset{}{\overset{K_d}{\rightleftharpoons}} PR \xrightarrow{k_{cat}} product$$

[a] P = P450; R = CPR.

first models of the functional P450 complex was a rigid cluster of multiple P450 molecules surrounding a single CPR molecule (4). However, rotational diffusion studies (6, 7), cross-linking efforts (8, 9), and catalytic studies with solubilized P450 and CPR (10−12) later favored a more dynamic mass action model whereby monomeric P450 and CPR were in equilibrium with a functional binary complex, as shown in Scheme 1. Predictions from this mechanism have influenced both the design and interpretation of studies elucidating the biological impact of P450 activity.

CYP2E1 activity is highly dependent on the composition of the functional complex. CYP2E1 plays a central role in the metabolism of a large number of small molecular weight compounds (molecular weight <100), such as aliphatic, aromatic, and halogenated hydrocarbons, many of which are solvents and industrial monomers and some of which are suspected to cause cancer (13). Although the most notable CYP2E1 substrate is ethanol, *p*-nitrophenol (pNP) is regarded as a typical model substrate (14). The ability to transform these compounds to products depends on the coupling of electron-transfer processes between CYP2E1 and redox partners, CPR and cyt b_5 (14). The mechanism by which the functional complex(es) form(s) for these prospective partners remains to be resolved. Unlike other P450s, cyt b_5 can even support certain reactions in the absence of CPR (15), further underscoring the complexity of the role of protein−protein interactions in CYP2E1 function. Poor coupling efficiency for CYP2E1 reactions leads to decreased transformation of organic substrates to products and the formation of reactive oxygen species, a precursor to oxidative stress. The biological significance of CYP2E1-induced oxidative stress has been implicated in alcohol-induced liver damage and roles in diabetes, obesity, fasting, cancer, and nonalcoholic steatohepatitis (reviewed in ref 16).

Due to the significance of protein−protein interactions in CYP2E1 activity, our goal in this study was to observe the effect of varied total concentrations of both proteins (CYP2E1 and CPR) on the overall catalytic activity of CYP2E1 toward the model substrate pNP. Because CPR is prone to degradation by contaminating proteases, we employed a proteolytically resistant form of reductase, CPR-K56Q, which eliminated a known site of cleavage (17, 18). Initially, we employed the strategy of Miwa et al. (12) and performed a series of catalytic titrations for CYP2E1 and CPR-K56Q under conditions of excess titrant. Nevertheless, the choice of titrant yielded contradictory parameters for a binary complex mechanism, and a Job plot at 400 nM indicated the presence of a higher order complex.

To reconcile these results, we eliminated titrant bias by expanding the experimental conditions and fit the data to models incorporating multiple complexes. For these experiments, both CPR and P450 were varied simultaneously, and neither protein was in very large excess. On the basis of reports by others (19, 20), we proposed CYP2E1 and CPR-K56Q could form binary, ternary, and quaternary complexes in the absence or presence of P450 and CPR homodimers.

Due to evidence for the binary functional complex, we required all models to include P450·CPR. For simplicity, we also assumed all complexes including both P450 and CPR to be catalytically active. The resulting 32 complexation models were used to perform global regression analysis of all pooled experimental data. Model discrimination analysis was performed on the basis of the second-order Akaike information criterion, which properly takes into account the fact that various fitting models contain a different number of adjustable model parameters. The approach enabled the ability to identify the most probable complexes present in the CYP2E1−CPR system.
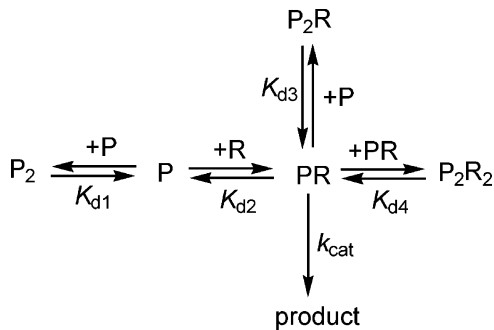
EXPERIMENTAL PROCEDURES

Materials. Components of the NADPH regenerating system (NADP$^+$, glucose 6-phosphate, torula yeast glucose-6-phosphate dehydrogenase) for catalytic assays were purchased from Sigma-Aldrich, as were dilauroyl-L-α-phosphatidylcholine, *p*-nitrophenol, *p*-nitrocatechol, 2-nitroresorcinol, bovine erythrocyte superoxide dismutase, and catalase. HPLC grade acetonitrile, trifluoroacetic acid, and other basic chemicals were purchased from Fisher Scientific (Houston, TX). Rabbit CYP2E1 and CPR-K56Q were expressed in *Escherichia coli* and purified to homogeneity using modifications of published protocols (18, 21).

Enzyme Assays. Initial reaction rates of CYP2E1-mediated oxidation of *p*-nitrophenol to *p*-nitrocatechol were determined by a high-throughput HPLC method developed in our laboratory (18). In brief, a 96-well 0.5 mL V-bottom assay block (Corning Inc., Corning, NY) was used to reconstitute CPR-K56Q-mediated CYP2E1 activity at appropriate protein concentrations. The reaction contained also 50 mM potassium phosphate, pH 7.4, 20 μM dilauroyl-α-L-phosphatidylcholine (DLPC), 250 μM pNP, 2 units/μL catalase, 0.04 μg/μL superoxide dismutase, and an NADPH regenerating system (2 microunits/μL glucose-6-phosphate dehydrogenase, 10 mM glucose 6-phosphate, 2 mM MgCl$_2$, 500 μM NADP$^+$). Superoxide dismutase and catalase were added to the reaction to scavenge reactive oxygen species (O$_2^{\bullet-}$ and H$_2$O$_2$), because these products of uncoupled catalytic complex(es) may inactivate CYP2E1, which would complicate the analyses of the data. Reactions were prepared in sets of eight to correspond to the eight wells for each column of the microplate. The strategy facilitated large-scale, simultaneous manipulation of samples with a multichannel pipettor. Following the addition of all components except NADP$^+$, the reactions in the assay block were incubated at 37 °C for 5 min. The reactions were initiated upon addition of NADP$^+$. At three time points, an aliquot was taken from the reaction, quenched with acetonitrile, and further analyzed by HPLC as described (18).

Catalytic Titrations. For a two-component system whereby only one functional complex forms, catalytic titrations are a commonly used method for obtaining apparent dissociation constants based on the observed reaction rate. The application of the approach has been discussed in detail elsewhere for the P450 system (22). For these studies, the concentration of one component was held constant (at concentrations equal to 15, 30, and 60 nM) while the second component served as a titrant varied at the following concentrations: 7.5, 15, 30, 60, 100, 200, 300, and 400 nM. The rates (ν) for pNP

Scheme 2: The Most Plausible Mechanism for Formation and Catalytic Activity of Functional Complexes between P450 and CPR[a]

[a] P = P450; R = CPR.

oxidation under those conditions were measured, plotted as a function of the variable component concentration, and fit to eq 1 using GraphPad Prism (SanDiego, CA) to yield the maximal rate (V_{max}) and the apparent dissociation constant, K_d. In eq 1, [P] is the total or analytic concentration of P450 and [R] is the total or analytic concentration of CPR.

$$\nu = V_{max} \frac{K_d + [P] + [R] - \{(K_d + [P] + [R])^2 - 4[P][R]\}^{1/2}}{2} \quad (1)$$

Because the reaction rate according to eq 1 presumably derives from a single 1:1 complex, we determined the apparent turnover number (k_{cat}) from a series of catalytic titrations at concentrations of the constant component held at 15, 30, and 60 nM. The concentration of the putative binary complex is directly proportional to V_{max}, according to eq 2.

$$V_{max} = k_{cat}[P450 \cdot CPR] \quad (2)$$

At V_{max} the system is saturated such that the concentration of the binary complex is defined by the concentration of the limiting component. We constructed linear plots V_{max} vs the total concentration of the fixed component and fit the data to a straight line through the origin using GraphPad Prism (San Diego, CA) to determine the k_{cat} value for the presumed binary functional complex.

Mathematical Models for P450−CPR Interactions. The mathematical models for the catalytic activity of the reconstituted P450 enzyme were represented as systems of simultaneous nonlinear algebraic equations for the mass balances of the component molecular species, according to a formalism described earlier (*1*). For example, for mechanism 14c shown in Scheme 2, the system of nonlinear equations is

$$[P]_{tot} = [P] + [PR] + 2[P_2R] + 2[P_2R_2] + 2[P_2] \quad (3a)$$

$$[R]_{tot} = [R] + [PR] + [P_2R] + 2[P_2R_2] \quad (3b)$$

where the subscript tot means total or analytical concentration and square brackets symbolize the concentrations at equilibrium. After substituting for the equilibrium concentrations of molecular complexes in terms of equilibrium constants (see Scheme 2), we obtain for mechanism 14c two nonlinear

algebraic equations (eqs 4a,b) for two unknowns, $[P]_{eq}$ and $[R]_{eq}$:

$$[P]_{tot} = [P] + [P][R]/K_{d2} + 2[P]^2[R]/K_{d2}K_{d3} + 2[P]^2[R]^2/K_{d2}K_{d4} + 2[P]^2/K_{d1} \quad (4a)$$

$$[R]_{tot} = [R] + [P][R]/K_{d2} + [P]^2[R]/K_{d2}K_{d3} + 2[P]^2[R]^2/K_{d2}K_{d4} \quad (4b)$$

Similar systems of simultaneous nonlinear algebraic equations were automatically derived by the data-fitting software package DynaFit (*23*) from a symbolic input shown in the Supporting Information. Each system of nonlinear equations, corresponding to the given mechanism, was iteratively solved within DynaFit by using a modification of the algorithm equil by I and Nancollas (*24*) based on the multidimensional Newton−Raphson method. Subsequently, the equilibrium concentrations of the molecular complexes were computed from the definition of the corresponding dissociation constants. For example, for model 14c we obtain

$$[PR] = [P][R]/K_{d2} \quad (5a)$$

$$[P_2R] = [P]^2[R]/K_{d2}K_{d3} \quad (5b)$$

$$[P_2R_2] = [P]^2[R]^2/K_{d2}K_{d4} \quad (5c)$$

$$[P_2] = [P]^2/K_{d1} \quad (5d)$$

Finally, the observed catalytic activity is modeled as the sum total of the catalytic activities of all reactive molecular complexes. In model 14c in Scheme 2, there is only one catalytically active complex. Therefore, eq 6 contains only a single term:

$$\nu = k_{cat}[PR] \quad (6)$$

Rate equations similar to those shown in eq 6 were automatically derived by DynaFit (*23*) for all 32 models (mechanism) in Table 2 and for additional mechanisms shown in Table 3.

Regression Analysis. Each mathematical model, for example, eq 6 for mechanism 14c, was fit to the available experimental data by using two different methods. First, a global nonlinear least-squares minimization technique, based on the differential evolution (DE) algorithm (*25*) was used to approximately locate the *global* least-squares minimum in the multidimensional parameter space. The DE algorithm is mathematically guaranteed to find the best possible nonlinear fit within a prescribed range of model parameters, regardless of the initial estimates. Our constraints for all model parameters (equilibrium constants and turnover numbers) spanned 12 orders of magnitude. Second, the approximate solution obtained by DE was further refined by the usual Levenberg−Marquardt nonlinear regression algorithm implemented in DynaFit (*23*).

Model Discrimination Analysis. The residual sum of squares for each candidate fitting model (see mechanisms 1 through 4 in Scheme 1), SSQ, was used to compute the second-order Akaike information criterion AIC_c, according to eq 7 (*26*). In eq 7, n_P is the number of adjustable model parameters (e.g., equilibrium constants and turnover numbers

appearing in the given model) and n_D is the number of data points.

$$AIC_c = -2 \log SSQ + 2n_P + \frac{2n_P(n_P + 1)}{n_D - n_P - 1} \quad (7)$$

To assess the plausibility of different candidate models, we used the heuristic criteria proposed by Burnham and Anderson (*26*). First, we ranked all models in order of increasing value of AIC_c. We then considered a candidate model as implausible if the difference between the AIC_c value for this particular model and the AIC_c value for the "best" model (characterized by the lowest AIC_c value) was larger than 10. An additional measure of model adequacy was the Akaike weight defined by eq 8 (*26*), where $\Delta AIC_c^{(i)}$ is the difference between the AIC_c value for the *i*th model being compared and the lowest AIC_c value seen among all *N* candidate models.

$$w_i = \frac{\exp\left(-\frac{1}{2}\Delta AIC_c^{(i)}\right)}{\displaystyle\sum_{i=1}^{N}\exp\left(-\frac{1}{2}\Delta AIC_c^{(i)}\right)} \quad (8)$$

RESULTS

Catalytic Titrations at Excess of Titrant. Similar to the approach adopted by Miwa et al. (*12*) for CYP2B1, we performed and analyzed a series of catalytic titrations to determine the apparent K_d for the putative binary complex and to assess the relationship between the binary complex concentration and the maximal rate of substrate turnover. In one set of experiments, we titrated 15, 30, and 60 nM CYP2E1 with increasing concentrations of CPR-K56Q to near saturation at 400 nM and measured the observed reaction rate for pNP oxidation, as shown in Figure 1, panel A. Unlike the original study (*12*), we additionally conducted a complementary set of experiments, whereby we held the concentration of CPR-K56Q constant and varied CYP2E1 (Figure 2, panel A). Initially, we analyzed each titration curve independently as described by others (*12*). These data were fit individually to eq 1 to determine the apparent dissociation constants (K_d) and maximal rates (V_{max}). The average of the K_d values for each set of titrations where either CPR-K56Q or CYP2E1 served as titrant is shown in Table 1. The binary complex mechanism predicts a linear correlation between V_{max} and the CYP2E1·CPR-K56Q concentration, with slope equal to the turnover number, k_{cat} (eq 2). Under near-saturating concentration of the varied component, the concentration for the putative binary complex is equal to the concentration of the constant component, based on the one-to-one correspondence between these equilibrium components in the mechanism (Scheme 1). Thus, we plotted the V_{max} as a function of CYP2E1 concentration for titrations with CPR-K56Q and vice versa for titrations with CYP2E1 (Figures 1 and 2, panel B). Both data sets were fit to a straight line forced through the origin to determine the respective turnover numbers in Table 1. To improve the precision of data analysis, we fit all three data sets globally to the binary complex mechanism shown in Scheme 1 using DynaFit (*23*) and compared the resulting K_d and V_{max} values from the
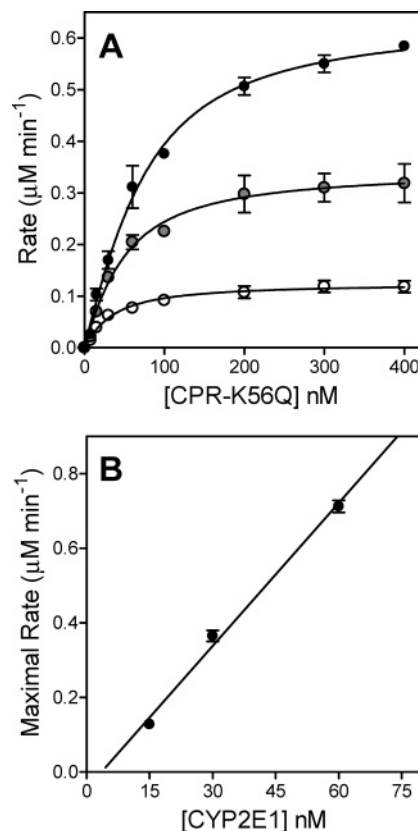

FIGURE 1: Catalytic titrations using CPR-K56Q as the titrant. (A) Reaction rates were plotted as a function of CPR-K56Q concentration. The reported values reflect the results from an average of two to four experiments including the standard deviation of the mean. The concentration of CYP2E1 in each titration was 15, 30, and 60 nM, as indicated by the white to black filling of the respective circles. The fitted line reflects the fit of each data set to a binding quadratic equation (eq 1). (B) The maximal rates from each titration were plotted as a function of the concentration of the limiting complex partner, CYP2E1, and then fit to a linear regression to determine k_{cat}.

respective methods. Although the resulting parameters were similar to those obtained by the traditional analysis of the data, there was at least a 2-fold drop in the formal standard error for the respective model parameters while using global analysis of the data (Table 1).

In both cases (independent or global analysis; see Table 1), the relationship between the observed reaction rates and the titrant concentrations conformed to the predictions based on assuming the simplest binary complex mechanism but yielded significantly different results depending on which component was held constant in the experiment and which component was varied. Regardless of the method of analysis, the titration of CYP2E1 with CPR-K56Q seemingly resulted in the formation of a functional complex, which displayed an approximate 2.5-fold lower affinity but ~50% higher activity than that predicted when CYP2E1 served as the titrant. Taken together, our results contradicted the predictions of the binary complex mechanism, because merely exchanging the constant component and the variable component in catalytic titrations seemed to produce fundamentally different properties for the putative 1:1 functional complex between CYP2E1 and CPR-K56Q.

Job Plot at 400 nM Total Protein Concentration. To determine the stoichiometry for the CYP2E1 and CPR-K56Q
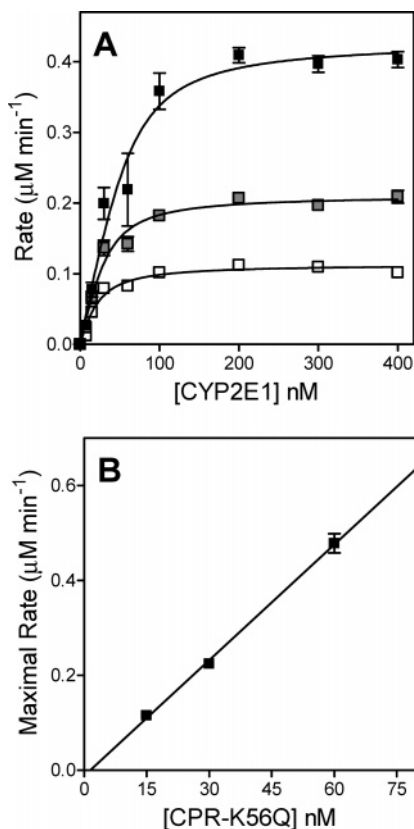
FIGURE 2: Catalytic titrations using CYP2E1 as the titrant. (A) Reaction rates were plotted as a function of CYP2E1 concentration. The reported values reflect the results from an average of two to four experiments including the standard deviation of the mean. The concentration of CPR-K56Q in each titration was 15, 30, and 60 nM, as indicated by the white to black filling of the respective squares. The fitted line reflects the fit of each data set to a binding quadratic equation (eq 1). (B) The maximal rates from each titration were plotted as a function of the concentration of the limiting complex partner, CPR-K56Q, and then fit to a linear regression to determine k_{cat}.

Table 1: Determination of Binary Complex Parameters Using either CPR-K56Q or CYP2E1 as the Titrant.

method of analysis	CPR-K56Q as titrant		CYP2E1 as titrant	
	K_d (nM)	k_{cat} (min^{-1})	K_d (nM)	k_{cat} (min^{-1})
independent[a]	30 ± 10	9.7 ± 1.2	12 ± 5	7.9 ± 0.2
global[b]	36 ± 3	10.7 ± 0.3	15.6 ± 1.4	7.2 ± 0.2

[a] K_d values were determined by averaging the results from the fit of each titration curve to the respective binding quadratic equation (eq 1). The turnover numbers, k_{cat}, were derived from the slope of the linear regression between V_{max} and the concentration of limiting complex partner as shown in Figures 1 and 2, panel B. [b] Parameters reflect the global fit of all three titration curves to a binary complex mechanism using the software DynaFit (23). The input data for this analysis are included in the Supporting Information.

complex(es), we performed a Job titration (27) at 400 nM total protein (P450 plus reductase), as described for CYP2B1 (12). The data were fit to a binary complex mechanism (Figure 3, dashed curve). If the reductase−cytochrome binding were strictly 1:1, the theoretically predicted maximum on the Job plot would be located at the center, at mole fraction $x_{P450} = 0.5$. Instead, the experimentally observed maximum is shifted toward $x_{P450} < 0.5$, indicating other than 1:1 molar ratio in at least one molecular complex being
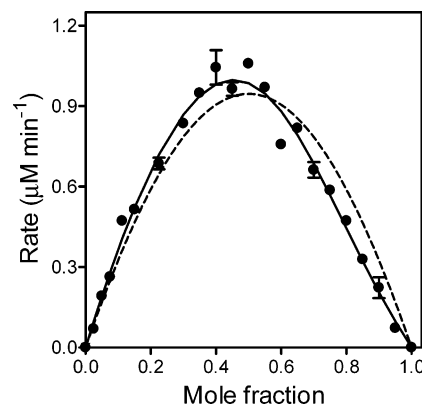

FIGURE 3: Job plot at a total protein concentration of 400 nM. The mole fraction (x) is defined by [CYP2E1]/([CYP2E1] + [CPR-K56Q]). Reaction rates were measured while CPR-K56Q and CYP2E1 concentrations were varied such that the total protein concentration remained at 400 nM. These data were fit to two different models using DynaFit (23). The dashed curve represents the best least-squares fit to the binary complex model (Scheme 1). The solid curve represents the fit to a model possessing a binary (P450·CPR) and ternary [P450·(CPR)$_2$] complex.

formed. These results unambiguously establish that a higher order molecular complex is present.

Global Analysis of Potential Complexation Mechanisms. To explain these observations, we developed a novel approach to identify the complexation mechanism for CYP2E1 and CPR-K56Q. As a first step, we generated a comprehensive data set to avoid bias from the choice of titrant (vide infra). Our comprehensive data set consisted of both components (P450 and CPR) being varied simultaneously over a wide range of concentrations, rather than being varied one at a time (as in catalytic titrations) or being varied such that the sum total of protein concentrations remains constant (as in the Job plot). We then globally fit these data to a variety of potential binding mechanisms and statistically analyzed the quality of the fits to select the most probable model.

Similar to the approach adopted by Hazai et al. (20), we proposed that CYP2E1 and CPR-K56Q could form binary (P450·CPR), ternary [(P450)$_2$·CPR and P450·(CPR)$_2$], and quaternary [(P450)$_2$·(CPR)$_2$] complexes in the absence or presence of P450 and CPR homodimers. Due to experimental support for the binary complex, we required the presence of the P450·CPR complex in all model mechanisms. To further limit the number of possible models, we assumed all complexes containing at least one P450 and one CPR molecule, respectively, were catalytically active. Altogether, there were 32 possible combinations of these complexes (Table 2). We did not consider alternate pathways to generate these complexes, because the equilibrium conditions for the system enabled only the ability to identify complexes, not the path through which they formed (28). The detailed description of the 32 reaction mechanisms is shown in the Supporting Information.

After fitting the data to all 32 possible binding mechanisms, we generated a corresponding Akaike information criterion (AIC$_c$) to describe statistically the quality of the respective fits. The models were ranked according to the difference in Akaike weights relative to the most probable model. To evaluate the plausibility of models, we employed the significance rules outlined by Burnham and Anderson

Table 2: Complete List of Binding Models Considered in This Study[a]

model	PR	P$_2$R	PR$_2$	P$_2$R$_2$	P$_2$	model	PR	P$_2$R	PR$_2$	P$_2$R$_2$	P$_2$
1	A					9	A				N
2	A	A				10	A	A			N
3	A		A			11	A		A		N
4	A	A	A			12	A	A	A		N
5	A			A		13	A			A	N
6	A	A		A		14	A	A		A	N
7	A		A	A		15	A		A	A	N
8	A	A	A	A	N	16	A	A	A	A	N

[a] The symbol A means that the given molecular complex is present and catalytically active. The symbol N means that the given complex is present but not catalytically active. Models 17 through 32 (not shown) are exactly identical to models 1 through 16, except for the fact that the reductase dimer (R$_2$) is also present.

Table 3: First Round of Discrimination between Candidate Mechanisms by Global Analysis[a]

model	PR	P$_2$R	PR$_2$	P$_2$R$_2$	P$_2$	R$_2$	SS$_{rel}$	ΔAIC$_c$	$w > 0.10$
13	A			A	N		1.094	0.0	0.259
14	A	A		A	N		1.069	1.6	0.116
15	A		A	A	N		1.064	1.0	0.160
32	A	A	A	A	N	N	1.000	0.1	0.248

[a] For an explanation of symbols A and N, see Table 2. SS$_{rel}$ = relative sum of squares; ΔAIC$_c$ = increase in the second-order Akaike information criterion (eq 7) relative to the best model (ΔAIC$_c$ = 0); w = Akaike weight (eq 8). Only models resulting in Akaike weight $w > 0.10$ (10% probability) are shown. For further explanation, see text.

Table 4: Second Round of Discrimination between Candidate Mechanisms by Global Analysis[a]

model	PR	P$_2$R	PR$_2$	P$_2$R$_2$	P$_2$	SS$_{rel}$	ΔAIC$_c$	$w > 0.10$
13	A			A	N	1.029	3.40	
13a	A			N	N	1.028	1.10	0.183
14	A	A		A	N	1.004	4.80	
14a	A	A		N	N	1.003	2.40	
14b	A	N		A	N	1.003	2.40	
14c	A	N		N	N	1.002	0.00	0.318
15	A		A	A	N	1.001	4.40	
15a	A		A	N	N	1.000	2.00	0.118
15b	A		N	A	N	1.043	7.40	
15c	A		N	N	N	1.028	3.30	

[a] For an explanation of symbols A and N, see Table 2. SS$_{rel}$ = relative sum of squares; ΔAIC$_c$ = increase in the second-order Akaike information criterion (eq 7) relative to the best model (ΔAIC$_c$ = 0); w = Akaike weight (eq 8). The Akaike weight is listed only for those models where $w > 0.10$ (10% probability). For further explanation, see text.

Table 5: Optimized Parameters for the Most Plausible Model 14c[a]

reaction	parameter	best-fit value	std error	lower limit	upper limit
2P ⇌ P$_2$	K_{d1}, μM	0.038	±0.052	0.0013	0.28
P + R ⇌ PR	K_{d2}, μM	0.021	±0.011	0.0044	0.041
PR + P ⇌ P$_2$R	K_{d3}, μM	0.37	±0.12	0.19	1.9
2PR ⇌ P$_2$R$_2$	K_{d4}, μM	0.041	±0.019	0.0036	0.070
PR → product	k_{cat}, min^{-1}	10.6	±0.6	9.7	11.9

[a] See Table 4 and Scheme 2 for model description. The limiting values were computed at a 90% confidence level by using the profile-t method of Bates and Watts (29).

(ref 26, p 70). Low AIC$_c$ values indicated comparatively high support for the given model. More specifically, there was substantial support for the given model when the ΔAIC$_c$ was between 0 and 2. Values between 4 and 7 signify considerably less support for the model, while a ΔAIC$_c$ of 10 or greater indicated essentially no support for the given model.

Identification of Plausible Complexation Models. In the first round of model discrimination analysis we compared 32 possible complexation models (mechanisms) shown in Table 2, while assuming all molecular complexes except the (P450)$_2$ and (CPR)$_2$ homodimers are catalytically active. Of these 32 possible models for complexation, only four (models 13, 14, 15, and 32) were associated with Akaike weights greater than 0.10 (corresponding to 10% statistical probability of the given model being correct). Numerical results for the four preferred models are summarized in Table 3. Model 32, involving all possible molecular complexes being formed simultaneously, produced an extremely large uncertainty of all model parameters (equilibrium constants and turnover numbers) and was excluded from further consideration. The three remaining preferred models shown in Table 3 (models 13, 14, and 15) all include the binary complex P450·CPR and the quaternary complex (P450)$_2$·(CPR)$_2$. Model 14 additionally includes the ternary complex (P450)$_2$·CPR, whereas model 15 includes the ternary complex P450·(CPR)$_2$.

While examining the best-fit parameters for models 13 through 15 (data not shown), we noted that all turnover numbers associated with molecular complexes other than the binary complex P450·CPR were extremely small, numerically approaching zero. This observation suggested that we perform a second round of model discrimination analysis, summarized in Table 4. Here we have modified models 13

through 15 such that all complexes appearing in each given mechanism, except the binary complex P450·CPR, were progressively rendered catalytically inactive. The results of model discrimination analysis (Table 4) show that in fact nominally the most plausible mechanism is represented by model 14c, in which only the binary complex P450·CPR is catalytically active but not the ternary complex (P450)$_2$·CPR or the quaternary complex (P450)$_2$·(CPR)$_2$, both of which are also formed. A close second in order of plausibility is model 13a, which is identical to model 14c except for the fact that the ternary complex (P450)$_2$·CPR is not formed at all.

Confidence Intervals for Model Parameters. Nonsymmetrical confidence intervals for all model parameters, at the 90% probability level, were computed by using the profile-t method of Bates and Watts (29). The results are summarized for nominally the most plausible model 14c in Table 5.

DISCUSSION

In this study, traditional approaches failed to explain the observed catalytic activity of CYP2E1, in dependence on the total concentration of added CPR-K56Q. Thus, we developed a novel approach to studying protein−protein interactions that revealed CYP2E1 and CPR-K56Q form multiple complexes rather than the expected single binary P450·CPR complex.

For the titrations with either CPR-K56Q or CYP2E1 as the titrant, the reaction rates and the titrant concentration seemingly followed the simplest 1:1 binding isotherm (Figures 1 and 2, panel A). The maximal rates from each of

the titration curves were linearly dependent on the concentration of the limiting complex partner, regardless of the choice of titrant (Figures 1 and 2, panel B). The low dissociation constant for the binary complex in each set of experiments is reasonable, based on similar reported values for titrations by other P450 systems (*12, 22, 30, 31*). Each data set viewed independently would support the contention that only a single functional complex forms between CPR-K56Q and CYP2E1. However, depending on which component was varied and which was held constant, the two subsets of the experimental data were mutually contradictory. With CPR-K56Q used as the titrant, the apparent K_d was 2.5-fold higher and the apparent k_{cat} was approximately 50% higher, compared to the data obtained with CYP2E1 as the titrant (Table 1). Thus, a reliance on simple titrations to study protein−protein interactions has led to contradictory conclusions.

To shed light on the inconsistencies resulting from the postulated 1:1 binding model, we generated a traditional Job plot (*27, 32*) to determine a possible presence of higher order complexes, characterized by stoichiometries other than 1:1. For this study, catalytic activity was measured as a function of the mole fraction for each complex partner at a constant total molar concentration of protein. The exclusive presence of a 1:1 binary complex between CYP2E1 and CPR-K56Q should yield a symmetrical parabola with a maximum at mole fraction (χ) exactly identical to 0.5, where the concentrations of P450 and CPR are the same. For CYP2E1 and CPR-K56Q, we found the maximum rate to be located clearly at $\chi < 0.5$ (Figure 3), indicating that a higher molecular order complex was in fact present. The simultaneous presence of a binary complex cannot be ruled out. For example, a binary complex could serve as an intermediate to forming a higher order complex.

Although the first reported Job plot for a P450 system was symmetrical (*12*), subsequent publications (*33, 34*) for the CYP2B1 system included asymmetrical curves, whereby the maxima for the reaction rates were less than a mole fraction of 0.5 as we observed for CYP2E1. The unexpected Job plot for CYP2B1 was independent of the type (*33, 34*) or concentration (*33*) of lipid present. Whereas the authors suggested the unexpected results were due to detergent contamination or protein aggregation, we interpret their results as early evidence of the actual molecular order of the P450 complex. Coupled with our findings for CYP2E1, these results for CYP2B1 suggest higher molecular order functional complexes may be a more common mechanism determining activities for P450s. Nevertheless, the strategy of relying on simple catalytic titrations, where one component concentration is held constant and the other varied, or a single Job plot to determine the mechanism of complexation is obviously not sufficient.

Despite the general acceptance of the binary complex mechanism, there is accumulating evidence in support of alternative functional complexes. The temperature dependence for P450 reduction by CPR provided early support for the presence of mobile and immobile populations of P450s. On the basis of the properties of reduction and known excess of P450s relative to CPR (*4*), the authors favored a functional complex in which 8−12 P450 molecules associated with an individual CPR molecule, which was in equilibrium with a mobile P450 population. The use of detergents to modulate protein−protein interactions provided

the first direct evidence for higher order functional complexes. On the basis of sedimentation and gel filtration studies, CYP1A2 (*35*) and CYP2B4 (*36*) formed pentamers that associated with CPR for optimal activity [(P450)₅·CPR]. CPR also formed dimers and other higher ordered complexes; however, low amounts of detergent dispersed the complexes, indicating CPR homooligomers were less stable than those for the P450s.

More recently, the binary complex model failed to explain activity from mixed P450 systems whereby two different P450s were coexpressed or reconstituted with CPR. Rather than simple competition as expected for a single binary functional complex, different P450 isoforms decreased, increased, or did not alter respective P450 activities (reviewed in ref *37*). To explain these observations, Backes et al. (*19*) proposed several alternate mechanisms including the traditional binary complex mechanism and compared the simulations of these mechanisms to correlate changes in protein concentration to activity. The most likely mechanism incorporated the generation of two functional complexes; each of the respective P450s associated with CPR to form a ternary [(P450)₂·CPR] complex, whose catalytic properties were distinct from an intermediary binary (P450·CPR) complex. Building on previous efforts, another proposal incorporated more elaborate complexation mechanisms (*20*) incorporating binary, ternary, and quaternary [(P450)₂·(CPR)₂] complexes formed from monomeric and dimeric P450s and CPR. The authors based the formation of these complexes on (a) the crystallization of some P450s and CPR as dimers and (b) the known self-association of P450 and CPR whereby the dimer is the simplest homooligomer.

Similar to the approach adopted by Hazai et al. (*20*), we proposed that multiple functional complexes were possible under our reaction conditions. Specifically, varying the concentrations of CYP2E1 and CPR-K56Q could result in the formation of binary (P450·CPR), ternary [(P450)₂·CPR and P450·(CPR)₂], and quaternary [(P450)₂·(CPR)₂] complexes in the absence or presence or P450 and CPR homodimers. Unlike the authors of the original study, we wanted to explore all possible combinations of complexes that could exist and discriminate between the corresponding models to identify the most likely one for the CYP2E1 system. Due to the experimental evidence for the binary complex, we required all models to possess the P450·CPR complex. To further simplify this effort, we assumed all active complexes contained at least one P450 and one CPR molecule, respectively. We did not consider the alternate pathways to generate complexes. As in other studies (*19, 38*), our system was at equilibrium, and therefore (*28*) we could not even in principle determine the path through which these complexes were generated. Our equilibrium binding studies could only reveal which complexes were most likely to be present under reaction conditions. A more in-depth understanding of the complexation would require further study. Altogether, there were 32 possible combinations of these complexes (Table 2).

An investigation of the possible complexation mechanisms required a suitable data set describing the system of interest. Rather than the choice of titrant causing the conflicting results with the initial sets of catalytic titrations, the conditions of the experiments likely introduced bias in the analysis. Titrations were unidirectional in that the titrant was added
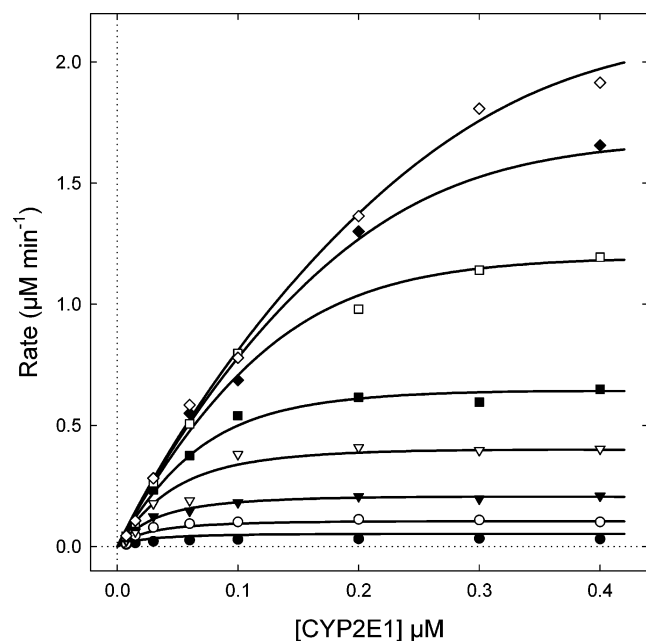
FIGURE 4: Pooled experimental data and the best-fit model (smooth curves) for model 14c defined in Table 3 and Scheme 2. CYP2E1 was varied from 7.5 to 400 nM. CPR concentrations were as follows: 7.5 nM (filled circles); 15 nM (open circles); 30 nM (filled triangles); 60 nM (open triangles); 100 nM (filled squares); 200 nM (open squares); 300 nM (filled diamonds); 400 nM (open diamonds). The best-fit model is represented by the system of simultaneous nonlinear algebraic equations (eqs 3−6), automatically derived and numerically solved by the software package DynaFit (*23*).

to excess with respect to the limiting complex partner, rather than any of the conditions in between these extremes. Our initial titrations and Job plot were limited subsets of data for the system, and, thus, limited the ability to assess the role of protein−protein interactions in regulating P450 activity. Similarly, reliance on the titration format and small data sets may explain why groups were not able to actually fit data from mixed P450 systems to possible complexation mechanisms (*19*, *31*, *38*, *39*).

As discussed by Beechem (*40*), global analysis of multidimensional data, for example, where multiple component concentrations are simultaneously varied and the entire superset is analyzed as a whole, is always more informative about the underlying biochemical mechanism, in comparison with trying to analyze individual subsets of data separately. For this study, we generated a two-dimensional data set where both P450 and CPR were simultaneously varied over a wide range of concentrations. In contrast, our preliminary experiments shown in Figures 1 and 2 only covered a narrow range of concentrations for either of the fixed components (P450 in Figure 1 or CPR in Figure 2). The experimental data we have collected are shown in Figure 4. These respective data sets provided an opportunity to determine which approach yielded the most useful information about the CYP2E1 system.

While previous efforts (*19*, *20*) *simulated* a limited number of proposed mechanisms, we *fit* our experimental data for the CYP2E1 system to 32 distinct models. Our ability to globally analyze the resulting data marked a significant step forward in understanding protein−protein interactions. The fit of each model provided values for parameters for models and corresponding confidence limits. From these fits, we also

generated a corresponding second-order Akaike information criterion [AIC_c (*26*)] to describe statistically the quality of the respective fits. On the basis of the differences between AIC_c for the proposed models (ΔAIC_c), we were able to identify a group of probable models for the CYP2E1 system. The results of this first round of model discrimination are summarized in Table 3.

Out of the 32 models examined, only four produced Akaike weight *w* (eq 8) higher than 0.10 (Table 3). This corresponds to the statistical probability higher than 10% that the given theoretical model could represent the "true" binding mechanism. Model 32 (last row in Table 3) was excluded from further consideration because it produced extremely high uncertainty in all adjustable model parameters (data not shown). This is not surprising, because model 32 encompasses *all* possible molecular interactions we allowed, with the simultaneous formation of six different P450·CPR complexes (four of which were presumed to be catalytically active), including the two homodimers. This degree of mechanistic complexity cannot be captured in our kinetic data. Therefore, we focused our attention on the three remaining mechanisms, models 13, 14, and 15 (see Table 3).

Models 13 through 15 are quite similar, in that they all involve the formation of the binary complex P450·CPR and the quaternary complex $(P450)_2 \cdot (CPR)_2$. The difference between the three mechanisms is a possible presence of either the ternary complex $(P450)_2 \cdot CPR$ (model 14) or the ternary complex $P450 \cdot (CPR)_2$ (model 15). We consider the similarity within this small family of plausible binding mechanisms encouraging: good evidence for the applicability of the Akaike information criterion in model discrimination (*26*). It would have been harder to understand if widely dissimilar mechanisms turned out equally plausible by AIC_c.

The best-fit values of the turnover numbers for the various complexes appearing in models 13 through 15 followed a consistent pattern, in that the numerical values of k_{cat} for all complexes, except the binary complex P450·CPR, were at least 3 orders of magnitude lower when compared to the k_{cat} for P450·CPR. We interpreted this result to mean that although the quaternary complex $(P450)_2 \cdot (CPR)_2$ is quite clearly formed, it is likely not to be catalytically active. The same applies to the homodimer $(P450)_2$ and to the ternary complexes $(P450)_2 \cdot CPR$ (model 14) or $P450 \cdot (CPR)_2$ (model 15). Therefore, in the next round of model discrimination analysis we rendered various P450·CPR complexes catalytically inactive, by assigning to them zero turnover number in the corresponding mathematical models. This generated eight candidate models (mechanisms) summarized in Table 4, along with the numerical results of model discrimination.

Nominally the most plausible model in Table 4 is represented by model 13b, shown in greater detail in Scheme 2. According to this mechanism, P450 forms a homodimer and additionally three different molecular complexes with CPR, namely, the catalytically active 1:1 complex P450·CPR and two catalytically inactive complexes, $(P450)_2 \cdot (CPR)_2$ and $(P450)_2 \cdot CPR$. The nonsymmetrical confidence intervals (*29*) for all model parameters (equilibrium constants and turnover numbers) are listed in Table 5. The overall stability of the ternary complex $(P450)_2 \cdot CPR$, as measured by the dissociation constant K_{d3} in Scheme 2, is significantly lower in comparison with the stability of both the binary complex (K_{d2}) and the quaternary complex (K_{d4}).

It is important to point out that, on the basis of *equilibrium* binding studies, we cannot unambiguously determine the pathway(s) by which the quaternary complex is formed, and in this sense the mechanism shown in Scheme 2 is only one of two possible pathways. In principle, the quaternary complex $(P450)_2 \cdot (CPR)_2$ could also be formed from the ternary complex $(P450)_2 \cdot CPR$ by associating an additional CPR molecule. However, this would imply that the association of the second molecule of CPR to the ternary complex $(P450)_2 \cdot CPR$ would have to be accompanied by strong *positive cooperativity*, given the relative values of $K_{d3} < K_{d4}$. For this reason we favor the mechanism shown in Scheme 2, according to which the quaternary complex is shown by dimerization of the heterodimer P450·CPR.

Concluding Remarks. Although we initially assumed recombinant CPR-K56Q and CYP2E1 formed a single functional complex, our study revealed that CYP2E1 catalytic activity derives from the presence of multiple complexes, which coexist under reaction conditions. The formation of these complexes resulted in an overall negative cooperative effect, whereby higher P450 concentrations suppressed activity. This effect may provide a toxicological advantage for the metabolism of CYP2E1 substrates when toxic products are generated. Through these efforts, we identified inherent shortcomings of traditional approaches to studying protein−protein interactions. To better understand the P450 system, we are the first to eliminate bias from reaction conditions and globally analyze data to identify the most probable complexes present in the system. Knowledge of these complexes provides an important foundation for further studies to confirm the presence of the complexes and to explore the role of their formation and contribution to overall enzymatic activity. The utility of our approach applies to any two-component system such as protein−ligand and protein−protein interactions, which provide the foundation for many biological processes.

ACKNOWLEDGMENT

We are thankful for helpful comments from a reviewer of the manuscript.

SUPPORTING INFORMATION AVAILABLE

The file includes the scripts (input data) for the DynaFit (*23*) software and the resulting output files. This material is available free of charge via the Internet at http://pubs.acs.org.

REFERENCES

1. Kuzmic, P. (2006) A generalized matrix formalism for steady state enzyme kinetics: Application to 17beta-HSD, *Mol. Cell. Endocrinol. 248*, 172−181.
2. Porter, T. D., and Coon, M. J. (1991) Cytochrome P-450: multiplicity of isoforms, substrates, and catalytic and regulatory mechanisms, *J. Biol. Chem. 266*, 13469−13472.
3. Hlavica, P., Schulze, J., and Lewis, D. F. (2003) Functional interaction of cytochrome P450 with its redox partners: a critical assessment and update of the topology of predicted contact regions, *Inorg. Biochem. 96*, 279−297.
4. Estabrook, R., Franklin, M. R., Cohen, B., Shigamatzu, A., and Hildebrandt, A. G. (1971) Biochemical and genetic factors influencing drug metabolism. Influence of hepatic microsomal mixed function oxidation reactions on cellular metabolic control, *Metabolism 20*, 187−199.
5. Watanabe, J., Asaka, Y., Fujimoto, S., and Kanamura, S. (1993) Densities of NADPH-ferrihemoprotein reductase and cytochrome
6. Gut, J., Richter, C., Cherry, R. J., Winterhalter, K. H., and Kawato, S. (1983) Rotation of cytochrome P-450: complex formation of cytochrome P-450 with NADPH-cytochrome P-450 reductase in liposomes demonstrated by combining protein rotation with antibody-induced cross-linking, *J. Biol. Chem. 258*, 8588−8594.
7. Schwarz, D., Pirrwitz, J., and Ruckpaul, K. (1982) Rotational diffusion of cytochrome P-450 in the microsomal membrane— evidence for a clusterlike organization from saturation transfer electron paramagnetic resonance spectroscopy, *Arch. Biochem. Biophys. 216*, 322−328.
8. Tamburini, P. P., MacFarquhar, S., and Schenkman, J. B. (1986) Evidence of binary complex formations between cytochrome P-450, cytochrome b_5, and NADPH-cytochrome P-450 reductase of hepatic microsomes, *Biochem. Biophys. Res. Commun. 134*, 519−526.
9. Nisimoto, Y., and Otsuka-Murakami, H. (1988) Cytochrome b_5, cytochrome *c*, and cytochrome P-450 interactions with NADPH-cytochrome P-450 reductase in phospholipid vesicles, *Biochemistry 27*, 5869−5876.
10. Yang, C. S., and Strickhart, F. S. (1975) Interactions between solubilized cytochrome P-450 and hepatic microsomes, *J. Biol. Chem. 250*, 7968−7972.
11. Yang, C. S., Strickhart, F. S., and Kicha, L. P. (1978) Interaction between NADPH-cytochrome P-450 reductase and hepatic microsomes, *Biochim. Biophys. Acta 509*, 326−337.
12. Miwa, G. T., West, S. B., Huang, M. T., and Lu, A. Y. (1979) Studies on the association of cytochrome P-450 and NADPH-cytochrome *c* reductase during catalysis in a reconstituted hydroxylating system, *J. Biol. Chem. 254*, 5695−5700.
13. Guengerich, F. P., Kim, D. H., and Iwasaki, M. (1991) Role of human cytochrome P-450 IIE1 in the oxidation of many low molecular weight cancer suspects, *Chem. Res. Toxicol. 4*, 168−79.
14. Ronis, M., Lindros, K. O., and Ingelman-Sundberg, M. (1996) The CYP2E1 subfamily, in *Cytochromes P450—metabolic and toxicological aspects* (Ioannides, C., Ed.) pp 211−239, CRC Press, Boca Raton, FL.
15. Yamazaki, H., Nakano, M., Gillam, E. M. J., Guengerich, F. P., and Shimada, T. (1996) Requirements for cytochrome b_5 in the oxidation of 7-ethoxycoumarin, chlorzoxazone, aniline, and *N*-nitrosodimethylamine by recombinant cytochrome P450 2E1 and by human liver microsomes, *Biochem. Pharmacol. 52*, 301−309.
16. Lewis, D. F., Bird, M. G., and Parke, D. V. (1997) Molecular modelling of CYP2E1 enzymes from rat, mouse and man: an explanation for species differences in butadiene metabolism and potential carcinogenicity, and rationalization of CYP2E substrate specificity, *Toxicology 118*, 93−113.
17. Bonina, T. A., Gilep, A. A., Estabrook, R. W., and Usanov, S. A. (2005) Engineering of proteolytically stable NADPH-cytochrome P450 reductase, *Biochemistry (Moscow) 70*, 357−365.
18. Collom, S. L., Jamakhandi, A. P., Tackett, A. J., Radominska-Pandya, A., and Miller, G. P. (2007) CYP2E1 active site residues in substrate recognition sequence 5 identified by photoaffinity labeling and homology modeling, *Arch. Biochem. Biophys. 459*, 59−69.
19. Backes, W. L., Batie, C. J., and Cawley, G. F. (1998) Interactions among P450 enzymes when combined in reconstituted systems: formation of a 2B4−1A2 complex with a high affinity for NADPH-cytochrome P450 reductase, *Biochemistry 37*, 12852−12859.
20. Hazai, E., Bikadi, Z., Simonyi, M., and Kupfer, D. (2005) Association of cytochrome P450 enzymes is a determining factor in their catalytic activity, *J. Comput.-Aided Mol. Des. 19*, 271−85.
21. Cheng, D., Kelley, R. W., Cawley, G. F., and Backes, W. L. (2004) High-level expression of recombinant rabbit cytochrome P450 2E1 in *Escherichia coli* C41 and its purification, *Protein Expression Purif. 33*, 66−71.
22. Bridges, A., Gruenke, L., Chang, Y.-T., Vakser, I. A., Loew, G., and Waskell, L. (1998) Identification of the binding site on cytochrome P450 2B4 for cytochrome b_5 and cytochrome P450 reductase, *J. Biol. Chem. 273*, 17036−17049.
23. Kuzmic, P. (1996) Program DYNAFIT for the analysis of enzyme kinetic data: Application to HIV proteinase, *Anal. Biochem. 237*, 260−273.

24. I, T.-P., and Nancollas, G. H. (1972) EQUIL−A general computational method for the calculation of solution equilibria, *Anal. Chem. 44*, 1940−1950.

25. Price, K. V., Storm, R. M., and Lampinen, J. A. (2005) *Differential Evolution−A Practical Approach to Global Optimization*, Springer-Verlag, Berlin and Heidelberg.

26. Burnham, K. B., and Anderson, D. R. (2002) *Model Selection and Multimodel Inference: A Practical Information-Theoretic Approach*, 2nd ed., Springer-Verlag, New York.

27. Job, P. (1928) Recherches sur la formation de complexes mineraux en solution, et sur leur stabilité, *Ann. Chim. (Paris) 9*, 113−203.

28. Denbigh, K. (1964) *The Principles of Chemical Equilibrium*, Cambridge University Press, Cambridge.

29. Bates, D. M., and Watts, D. G. (1988) *Nonlinear Regression Analysis and its Applications*, Wiley, New York.

30. Kaminsky, L. S., Lee, J. J., and Guengerich, F. P. (1985) Interactions of cytochromes P-450 and NADPH-cytochrome P-450 reductase, in *Abstracts, Fourth International Symposium on Comparative Biochemistry* pp 43, Beerse, Belgium.

31. Kelley, R. W., Reed, J. R., and Backes, W. L. (2005) Effects of ionic strength on the functional interactions between CYP2B4 and CYP1A2, *Biochemistry 44*, 2632−2641.

32. Huang, C. Y. (1982) Determination of binding stoichiometry by the continuous variation method: the Job plot, *Methods Enzymol. 87*, 509−525.

33. Miwa, G. T., and Lu, A. Y. H. (1981) Studies on the stimulation of cytochrome P-450-dependent monooxygenase activity by dilauroylphosphatidylcholine, *Arch. Biochem. Biophys. 211*, 454−458.

34. Miwa, G. T., and Lu, A. Y. H. (1984) The association of cytochrome P-450 and NADPH-cytochrome P-450 reductase in phospholipid membranes, *Arch. Biochem. Biophys. 234*, 161−166.

35. Sevrukova, I. F., Kanaeva, I. P., Koen, Y. M., Samenkova, N. F., Bachmanova, G. I., and Archakov, A. I. (1994) Catalytic activity of cytochrome P4501A2 in reconstituted system with Emulgen 913, *Arch. Biochem. Biophys. 311*, 133−143.

36. Dean, W. L., and Gray, R. D. (1982) Relationship between state of aggregation and catalytic activity for cytochrome P-450LM2 and NADPH-cytochrome P-450 reductase, *J. Biol. Chem. 257*, 14679−14685.

37. Backes, W. L., and Kelley, R. W. (2003) Organization of multiple cytochrome P450s with NADPH-cytochrome P450 reductase in membranes, *Pharmacol. Ther. 98*, 221−233.

38. Hazai, E., and Kupfer, D. (2005) Interactions between Cyp2C9 and Cyp2C19 in reconstituted binary systems influence their catalytic activity: Possible rationale for the inability of Cyp2C19 to catalyze methoxychlor demethylation in human liver microsomes, *Drug Metab. Dispos. 33*, 157−164.

39. Davydov, D. R., Petushkova, N. A., Bobrovnikova, E. V., Knyushko, T. V., and Dansette, P. (2001) Association of cytochromes P450 1A2 and 2B4: are the interactions between different P450 species involved in the control of the monooxygenase activity and coupling?, *Adv. Exp. Med. Biol. 500*, 335−338.

40. Beechem, J. M. (1992) Global analysis of biochemical and biophysical data, *Methods Enzymol. 210*, 37−54.

SUPPLEMENTARY INFORMATION

Global Analysis of Protein-Protein Interactions Reveals

Multiple CYP2E1–Reductase Complexes[†]

Arvind P. Jamakhandi[‡], Petr Kuzmic[§], Daniel E. Sanders[‡], and Grover P. Miller[‡,*]

[‡]Department of Biochemistry and Molecular Biology, University of Arkansas for

Medical Sciences, Little Rock, AR 72205, USA

[§]BioKin, Ltd, Pullman, WA 99163, USA

CONTENTS

DynaFit Script and Experimental Data - Model Discrimination #1

```
;_____

[task]

   data = equilibria
   task = fit
   model = PR* ?

[components]

   P, R

[mechanism]

   P + R <===> P.R        :      Kpr     dissoc

[constants]

   Kpr = 0.1 ?

[responses]

   P.R = 10 ?

[concentrations]

[data]

    variable     P, R
    set          alldata

[output]

    directory   ./output/models-round-1

;_____

[task]

   data = equilibria
   task = fit
   model = PR*-P2R* ?

[mechanism]

   P + R <===> P.R                 :      Kpr     dissoc
   P.R + P <===> P.P.R             :      Kppr    dissoc

[constants]
```

```
   Kpr = 0.1 ?
   Kppr = 0.1 ?

[responses]

   P.R = 10 ?
   P.P.R = 10 ?

;_____

[task]

   data = equilibria
   task = fit
   model = PR*-PR2* ?

[mechanism]

   P + R <===> P.R                 :      Kpr    dissoc
   P.R + R <===> P.R.R             :      Kprr   dissoc

[constants]

   Kpr = 0.1 ?
   Kprr = 0.1 ?

[responses]

   P.R = 10 ?
   P.R.R = 10 ?

;_____

[task]

   data = equilibria
   task = fit
   model = PR*-PR2*-P2R* ?

[mechanism]

   P + R <===> P.R                 :      Kpr    dissoc
   P.R + R <===> P.R.R             :      Kprr   dissoc
   P.R + P <===> P.P.R             :      Kppr   dissoc

[constants]

   Kpr = 0.1 ?
   Kprr = 0.1 ?
   Kppr = 0.1 ?

[responses]

   P.R = 10 ?
   P.R.R = 10 ?
   P.P.R = 10 ?
```

```
;_____

[task]

   data = equilibria
   task = fit
   model = PR*-P2R2* ?

[mechanism]

   P + R <===> P.R                 :      Kpr    dissoc
   P.R + P.R <===> P.R.P.R         :      Kprpr  dissoc

[constants]

   Kpr = 0.1 ?
   Kprpr = 0.1 ?

[responses]

   P.R = 10 ?
   P.R.P.R = 10 ?
;_____

[task]

   data = equilibria
   task = fit
   model = PR*-P2R*-P2R2* ?

[mechanism]

   P + R <===> P.R                 :      Kpr    dissoc
   P.R + P <===> P.P.R             :      Kppr   dissoc
   P.P.R + R <===> P.R.P.R         :      Kprpr  dissoc

[constants]

   Kpr = 0.1 ?
   Kppr = 0.1 ?
   Kprpr = 0.1 ?

[responses]

   P.R = 10 ?
   P.P.R = 10 ?
   P.R.P.R = 10 ?
;_____

[task]

   data = equilibria
   task = fit
   model = PR*-PR2*-P2R2* ?

[mechanism]
```

```
   P + R <===> P.R                  :      Kpr    dissoc
   P.R + R <===> P.R.R              :      Kprr   dissoc
   P.R.R + P <===> P.R.P.R          :      Kprpr  dissoc

[constants]

   Kpr = 0.1 ?
   Kprr = 0.1 ?
   Kprpr = 0.1 ?

[responses]

   P.R = 10 ?
   P.R.R = 10 ?
   P.R.P.R = 10 ?
;_____

[task]

   data = equilibria
   task = fit
   model = PR*-P2R*-PR2*-P2R2* ?

[mechanism]

   P + R <===> P.R                  :      Kpr    dissoc
   P.R + P <===> P.P.R              :      Kppr   dissoc
   P.R + R <===> P.R.R              :      Kprr   dissoc
   P.R.R + P <===> P.R.P.R          :      Kprpr  dissoc

[constants]

   Kpr = 0.1 ?
   Kppr = 0.1 ?
   Kprr = 0.1 ?
   Kprpr = 0.1 ?

[responses]

   P.R = 10 ?
   P.P.R = 10 ?
   P.R.R = 10 ?
   P.R.P.R = 10 ?
;_____

[task]

   data = equilibria
   task = fit
   model = PR*-P2 ?

[components]

   P, R

[mechanism]
```

```
   P + R <===> P.R         :      Kpr    dissoc
   P + P <===> P.P         :      Kpp    dissoc

[constants]

   Kpr = 0.1 ?
   Kpp = 0.1 ?

[responses]

   P.R = 10 ?

;_____

[task]

   data = equilibria
   task = fit
   model = PR*-P2R*-P2 ?

[mechanism]

   P + R <===> P.R              :      Kpr    dissoc
   P.R + P <===> P.P.R          :      Kppr   dissoc
   P + P <===> P.P              :      Kpp    dissoc

[constants]

   Kpr = 0.1 ?
   Kppr = 0.1 ?
   Kpp = 0.1 ?

[responses]

   P.R = 10 ?
   P.P.R = 10 ?

;_____

[task]

   data = equilibria
   task = fit
   model = PR*-PR2*-P2 ?

[mechanism]

   P + R <===> P.R              :      Kpr    dissoc
   P.R + R <===> P.R.R          :      Kprr   dissoc
   P + P <===> P.P              :      Kpp    dissoc

[constants]

   Kpr = 0.1 ?
   Kprr = 0.1 ?
   Kpp = 0.1 ?
```

```
[responses]

   P.R = 10 ?
   P.R.R = 10 ?


;_____


[task]

   data = equilibria
   task = fit
   model = PR*-PR2*-P2R*-P2 ?

[mechanism]

   P + R <===> P.R                :     Kpr    dissoc
   P.R + R <===> P.R.R            :     Kprr   dissoc
   P.R + P <===> P.P.R            :     Kppr   dissoc
   P + P <===> P.P                :     Kpp    dissoc

[constants]

   Kpr = 0.1 ?
   Kprr = 0.1 ?
   Kppr = 0.1 ?
   Kpp = 0.1 ?

[responses]

   P.R = 10 ?
   P.R.R = 10 ?
   P.P.R = 10 ?
;_____


[task]

   data = equilibria
   task = fit
   model = PR*-P2R2*-P2 ?

[mechanism]

   P + R <===> P.R                :     Kpr    dissoc
   P.R + P.R <===> P.R.P.R        :     Kprpr  dissoc
   P + P <===> P.P                :     Kpp    dissoc

[constants]

   Kpr = 0.1 ?
   Kprpr = 0.1 ?
   Kpp = 0.1 ?

[responses]

   P.R = 10 ?
   P.R.P.R = 10 ?
;_____
```

```
[task]

   data = equilibria
   task = fit
   model = PR*-P2R*-P2R2*-P2 ?

[mechanism]

   P + R <===> P.R                 :      Kpr    dissoc
   P.R + P <===> P.P.R             :      Kppr   dissoc
   P.P.R + R <===> P.R.P.R         :      Kprpr  dissoc
   P + P <===> P.P                 :      Kpp    dissoc

[constants]

   Kpr = 0.1 ?
   Kppr = 0.1 ?
   Kprpr = 0.1 ?
   Kpp = 0.1 ?

[responses]

   P.R = 10 ?
   P.P.R = 10 ?
   P.R.P.R = 10 ?
;_____

[task]

   data = equilibria
   task = fit
   model = PR*-PR2*-P2R2*-P2 ?

[mechanism]

   P + R <===> P.R                 :      Kpr    dissoc
   P.R + R <===> P.R.R             :      Kprr   dissoc
   P.R.R + P <===> P.R.P.R         :      Kprpr  dissoc
   P + P <===> P.P                 :      Kpp    dissoc

[constants]

   Kpr = 0.1 ?
   Kprr = 0.1 ?
   Kprpr = 0.1 ?
   Kpp = 0.1 ?

[responses]

   P.R = 10 ?
   P.R.R = 10 ?
   P.R.P.R = 10 ?
;_____

[task]
```

```
   data = equilibria
   task = fit
   model = PR*-P2R*-PR2*-P2R2*-P2 ?

[mechanism]

   P + R <===> P.R                 :     Kpr    dissoc
   P.R + P <===> P.P.R             :     Kppr   dissoc
   P.R + R <===> P.R.R             :     Kprr   dissoc
   P.R.R + P <===> P.R.P.R         :     Kprpr  dissoc
   P + P <===> P.P                 :     Kpp    dissoc

[constants]

   Kpr = 0.1 ?
   Kppr = 0.1 ?
   Kprr = 0.1 ?
   Kprpr = 0.1 ?
   Kpp = 0.1 ?

[responses]

   P.R = 10 ?
   P.P.R = 10 ?
   P.R.R = 10 ?
   P.R.P.R = 10 ?
;_____

[task]

   data = equilibria
   task = fit
   model = PR*-R2 ?

[components]

   P, R

[mechanism]

   P + R <===> P.R        :     Kpr    dissoc
   R + R <===> R.R        :     Krr    dissoc

[constants]

   Kpr = 0.1 ?
   Krr = 0.1 ?

[responses]

   P.R = 10 ?

;_____

[task]

   data = equilibria
```

```
   task = fit
   model = PR*-P2R*-R2 ?

[mechanism]

   P + R <===> P.R                :    Kpr    dissoc
   P.R + P <===> P.P.R            :    Kppr   dissoc
   R + R <===> R.R                :    Krr    dissoc

[constants]

   Kpr = 0.1 ?
   Kppr = 0.1 ?
   Krr = 0.1 ?

[responses]

   P.R = 10 ?
   P.P.R = 10 ?

;_____

[task]

   data = equilibria
   task = fit
   model = PR*-PR2*-R2 ?

[mechanism]

   P + R <===> P.R                :    Kpr    dissoc
   P.R + R <===> P.R.R            :    Kprr   dissoc
   R + R <===> R.R                :    Krr    dissoc

[constants]

   Kpr = 0.1 ?
   Kprr = 0.1 ?
   Krr = 0.1 ?

[responses]

   P.R = 10 ?
   P.R.R = 10 ?

;_____

[task]

   data = equilibria
   task = fit
   model = PR*-PR2*-P2R*-R2 ?

[mechanism]

   P + R <===> P.R                :    Kpr    dissoc
   P.R + R <===> P.R.R            :    Kprr   dissoc
```

```
   P.R + P  <===> P.P.R            :      Kppr   dissoc
   R + R    <===> R.R              :      Krr    dissoc

[constants]

   Kpr  = 0.1 ?
   Kprr = 0.1 ?
   Kppr = 0.1 ?
   Krr  = 0.1 ?

[responses]

   P.R   = 10 ?
   P.R.R = 10 ?
   P.P.R = 10 ?
;_____

[task]

   data = equilibria
   task = fit
   model = PR*-P2R2*-R2 ?

[mechanism]

   P + R    <===> P.R              :      Kpr    dissoc
   P.R + P.R <===> P.R.P.R         :      Kprpr  dissoc
   R + R    <===> R.R              :      Krr    dissoc

[constants]

   Kpr   = 0.1 ?
   Kprpr = 0.1 ?
   Krr   = 0.1 ?

[responses]

   P.R     = 10 ?
   P.R.P.R = 10 ?
;_____

[task]

   data = equilibria
   task = fit
   model = PR*-P2R*-P2R2*-R2 ?

[mechanism]

   P + R    <===> P.R              :      Kpr    dissoc
   P.R + P  <===> P.P.R            :      Kppr   dissoc
   P.P.R + R <===> P.R.P.R         :      Kprpr  dissoc
   R + R    <===> R.R              :      Krr    dissoc

[constants]

   Kpr  = 0.1 ?
```

```
   Kppr = 0.1 ?
   Kprpr = 0.1 ?
   Krr = 0.1 ?

[responses]

   P.R = 10 ?
   P.P.R = 10 ?
   P.R.P.R = 10 ?
;_____

[task]

   data = equilibria
   task = fit
   model = PR*-PR2*-P2R2*-R2 ?

[mechanism]

   P + R <===> P.R              :     Kpr    dissoc
   P.R + R <===> P.R.R          :     Kprr   dissoc
   P.R.R + P <===> P.R.P.R      :     Kprpr  dissoc
   R + R <===> R.R              :     Krr    dissoc

[constants]

   Kpr = 0.1 ?
   Kprr = 0.1 ?
   Kprpr = 0.1 ?
   Krr = 0.1 ?

[responses]

   P.R = 10 ?
   P.R.R = 10 ?
   P.R.P.R = 10 ?
;_____

[task]

   data = equilibria
   task = fit
   model = PR*-P2R*-PR2*-P2R2*-R2 ?

[mechanism]

   P + R <===> P.R              :     Kpr    dissoc
   P.R + P <===> P.P.R          :     Kppr   dissoc
   P.R + R <===> P.R.R          :     Kprr   dissoc
   P.R.R + P <===> P.R.P.R      :     Kprpr  dissoc
   R + R <===> R.R              :     Krr    dissoc

[constants]

   Kpr = 0.1 ?
   Kppr = 0.1 ?
   Kprr = 0.1 ?
```

```
   Kprpr = 0.1 ?
   Krr = 0.1 ?

[responses]

   P.R = 10 ?
   P.P.R = 10 ?
   P.R.R = 10 ?
   P.R.P.R = 10 ?
;_____

[task]

   data = equilibria
   task = fit
   model = PR*-P2-R2 ?

[components]

   P, R

[mechanism]

   P + R <===> P.R        :     Kpr    dissoc
   P + P <===> P.P        :     Kpp    dissoc
   R + R <===> R.R        :     Krr    dissoc

[constants]

   Kpr = 0.1 ?
   Kpp = 0.1 ?
   Krr = 0.1 ?

[responses]

   P.R = 10 ?

;_____

[task]

   data = equilibria
   task = fit
   model = PR*-P2R*-P2-R2 ?

[mechanism]

   P + R <===> P.R              :     Kpr    dissoc
   P.R + P <===> P.P.R          :     Kppr   dissoc
   P + P <===> P.P              :     Kpp    dissoc
   R + R <===> R.R              :     Krr    dissoc

[constants]

   Kpr = 0.1 ?
   Kppr = 0.1 ?
   Kpp = 0.1 ?
```

```
   Krr = 0.1 ?

[responses]

   P.R = 10 ?
   P.P.R = 10 ?

;_____

[task]

   data = equilibria
   task = fit
   model = PR*-PR2*-P2-R2 ?

[mechanism]

   P + R <===> P.R                    :      Kpr    dissoc
   P.R + R <===> P.R.R                :      Kprr   dissoc
   P + P <===> P.P             :      Kpp    dissoc
   R + R <===> R.R             :      Krr    dissoc

[constants]

   Kpr = 0.1 ?
   Kprr = 0.1 ?
   Kpp = 0.1 ?
   Krr = 0.1 ?

[responses]

   P.R = 10 ?
   P.R.R = 10 ?

;_____

[task]

   data = equilibria
   task = fit
   model = PR*-PR2*-P2R*-P2-R2 ?

[mechanism]

   P + R <===> P.R                    :      Kpr    dissoc
   P.R + R <===> P.R.R                :      Kprr   dissoc
   P.R + P <===> P.P.R                :      Kppr   dissoc
   P + P <===> P.P             :      Kpp    dissoc
   R + R <===> R.R             :      Krr    dissoc

[constants]

   Kpr = 0.1 ?
   Kprr = 0.1 ?
   Kppr = 0.1 ?
   Kpp = 0.1 ?
   Krr = 0.1 ?
```

```
[responses]

   P.R = 10 ?
   P.R.R = 10 ?
   P.P.R = 10 ?
;_____

[task]

   data = equilibria
   task = fit
   model = PR*-P2R2*-P2-R2 ?

[mechanism]

   P + R <===> P.R                 :     Kpr    dissoc
   P.R + P.R <===> P.R.P.R         :     Kprpr  dissoc
   P + P <===> P.P                 :     Kpp    dissoc
   R + R <===> R.R                 :     Krr    dissoc

[constants]

   Kpr = 0.1 ?
   Kprpr = 0.1 ?
   Kpp = 0.1 ?
   Krr = 0.1 ?

[responses]

   P.R = 10 ?
   P.R.P.R = 10 ?
;_____

[task]

   data = equilibria
   task = fit
   model = PR*-P2R*-P2R2*-P2-R2 ?

[mechanism]

   P + R <===> P.R                 :     Kpr    dissoc
   P.R + P <===> P.P.R             :     Kppr   dissoc
   P.P.R + R <===> P.R.P.R         :     Kprpr  dissoc
   P + P <===> P.P                 :     Kpp    dissoc
   R + R <===> R.R                 :     Krr    dissoc

[constants]

   Kpr = 0.1 ?
   Kppr = 0.1 ?
   Kprpr = 0.1 ?
   Kpp = 0.1 ?
   Krr = 0.1 ?

[responses]
```

```
    P.R = 10 ?
    P.P.R = 10 ?
    P.R.P.R = 10 ?
;_____

[task]

    data = equilibria
    task = fit
    model = PR*-PR2*-P2R2*-P2-R2 ?

[mechanism]

    P + R <===> P.R                :     Kpr    dissoc
    P.R + R <===> P.R.R            :     Kprr   dissoc
    P.R.R + P <===> P.R.P.R        :     Kprpr  dissoc
    P + P <===> P.P                :     Kpp    dissoc
    R + R <===> R.R                :     Krr    dissoc

[constants]

    Kpr = 0.1 ?
    Kprr = 0.1 ?
    Kprpr = 0.1 ?
    Kpp = 0.1 ?
    Krr = 0.1 ?

[responses]

    P.R = 10 ?
    P.R.R = 10 ?
    P.R.P.R = 10 ?
;_____

[task]

    data = equilibria
    task = fit
    model = PR*-P2R*-PR2*-P2R2*-P2-R2 ?

[mechanism]

    P + R <===> P.R                :     Kpr    dissoc
    P.R + P <===> P.P.R            :     Kppr   dissoc
    P.R + R <===> P.R.R            :     Kprr   dissoc
    P.R.R + P <===> P.R.P.R        :     Kprpr  dissoc
    P + P <===> P.P                :     Kpp    dissoc
    R + R <===> R.R                :     Krr    dissoc

[constants]

    Kpr = 0.1 ?
    Kppr = 0.1 ?
    Kprr = 0.1 ?
    Kprpr = 0.1 ?
    Kpp = 0.1 ?
```

```
   Krr = 0.1 ?

[responses]

   P.R = 10 ?
   P.P.R = 10 ?
   P.R.R = 10 ?
   P.R.P.R = 10 ?


;_____

[set:alldata]

P_tot R_tot rate
======    ======       =======

; Constant [R] = 0.0075, variable [P]

0.0075     0.0075      0.00776
0.0150     0.0075      0.01392
0.0300     0.0075      0.01849
0.0600     0.0075      0.02508
0.1000     0.0075      0.02651
0.2000     0.0075      0.02994
0.3000     0.0075      0.03101
0.4000     0.0075      0.02843
0.0075     0.0075      0.00894
0.0150     0.0075      0.01624
0.0300     0.0075      0.02498
0.0600     0.0075      0.02820
0.1000     0.0075      0.03220
0.2000     0.0075      0.03354
0.3000     0.0075      0.03636
0.4000     0.0075      0.03444

; Constant [R] = 0.0150, variable [P]

0.0075     0.0150      0.01078
0.0150     0.0150      0.04981
0.0300     0.0150      0.08317
0.0600     0.0150      0.09133
0.1000     0.0150      0.10090
0.2000     0.0150      0.10750
0.3000     0.0150      0.10700
0.4000     0.0150      0.09316
0.0075     0.0150      0.01415
0.0150     0.0150      0.04119
0.0300     0.0150      0.07528
0.0600     0.0150      0.09700
0.1000     0.0150      0.10240
0.2000     0.0150      0.11680
0.3000     0.0150      0.11200
0.4000     0.0150      0.11050

; Constant [R] = 0.0300, variable [P]

0.0075     0.0300      0.02263
```

```
0.0150      0.0300      0.07508
0.0300      0.0300      0.12210
0.0600      0.0300      0.15240
0.1000      0.0300      0.18510
0.2000      0.0300      0.20000
0.3000      0.0300      0.19380
0.4000      0.0300      0.20000
0.0075      0.0300      0.02529
0.0150      0.0300      0.07633
0.0300      0.0300      0.12580
0.0600      0.0300      0.14090
0.1000      0.0300      0.17940
0.2000      0.0300      0.21380
0.3000      0.0300      0.19970
0.4000      0.0300      0.21780

; Constant [R] = 0.0600, variable [P]

0.0075      0.0600      0.02419
0.0150      0.0600      0.05593
0.0300      0.0600      0.17880
0.0600      0.0600      0.19190
0.1000      0.0600      0.38380
0.2000      0.0600      0.41980
0.3000      0.0600      0.40820
0.4000      0.0600      0.41400
0.0075      0.0600      0.02915
0.0150      0.0600      0.06719
0.0300      0.0600      0.17680
0.0600      0.0600      0.18680
0.1000      0.0600      0.37670
0.2000      0.0600      0.39840
0.3000      0.0600      0.38470
0.4000      0.0600      0.39150

; Constant [R] = 0.1000, variable [P]

0.0075      0.1000      0.03527
0.0150      0.1000      0.07973
0.0300      0.1000      0.24090
0.0600      0.1000      0.37680
0.1000      0.1000      0.58850
0.2000      0.1000      0.63490
0.3000      0.1000      0.60490
0.4000      0.1000      0.64860
0.0075      0.1000      0.04025
0.0150      0.1000      0.08718
0.0300      0.1000      0.22710
0.0600      0.1000      0.37440
0.1000      0.1000      0.49120
0.2000      0.1000      0.59710
0.3000      0.1000      0.58710
0.4000      0.1000      0.64880

; Constant [R] = 0.2000, variable [P]

0.0075      0.2000      0.04323
```

```
0.0150      0.2000      0.09872
0.0300      0.2000      0.27430
0.0600      0.2000      0.48950
0.1000      0.2000      0.80310
0.2000      0.2000      0.96650
0.3000      0.2000      1.17800
0.4000      0.2000      1.19700
0.0075      0.2000      0.04303
0.0150      0.2000      0.09348
0.0300      0.2000      0.25100
0.0600      0.2000      0.52360
0.1000      0.2000      0.79180
0.2000      0.2000      0.99280
0.3000      0.2000      1.10400
0.4000      0.2000      1.19100

; Constant [R] = 0.3000, variable [P]

0.0075      0.3000      0.04482
0.0150      0.3000      0.10260
0.0300      0.3000      0.28060
0.0600      0.3000      0.53340
0.1000      0.3000      0.67150
0.2000      0.3000      1.27700
0.3000      0.3000      1.35500
0.4000      0.3000      1.67600
0.0075      0.3000      0.04380
0.0150      0.3000      0.11200
0.0300      0.3000      0.28430
0.0600      0.3000      0.56690
0.1000      0.3000      0.70200
0.2000      0.3000      1.32400
0.3000      0.3000      1.40500
0.4000      0.3000      1.63600

; Constant [R] = 0.4000, variable [P]

0.0075      0.4000      0.04410
0.0150      0.4000      0.10570
0.0300      0.4000      0.28690
0.0600      0.4000      0.57520
0.1000      0.4000      0.75220
0.2000      0.4000      1.31700
0.3000      0.4000      1.83200
0.4000      0.4000      1.94900
0.0075      0.4000      0.04505
0.0150      0.4000      0.10760
0.0300      0.4000      0.27610
0.0600      0.4000      0.59340
0.1000      0.4000      0.80600
0.2000      0.4000      1.41100
0.3000      0.4000      1.78300
0.4000      0.4000      1.88000

[end]
```

Results - Model Discrimination #1

Minimum sum of squares = 0.17464

	model	nD	nP	SSrel	AICc	Δ AICc	weight
[1]	PR*	128	2	4.537	-23.6	175.6	0.000
[2]	PR*-P2R*	128	4	1.775	-139.4	59.8	0.000
[3]	PR*-PR2*	128	4	1.450	-165.3	33.9	0.000
[4]	PR*-PR2*-P2R*	128	6	1.188	-186.4	12.8	0.000
[5]	PR*-P2R2*	128	4	2.202	-111.8	87.3	0.000
[6]	PR*-P2R*-P2R2*	128	6	1.173	-188.0	11.2	0.001
[7]	PR*-PR2*-P2R2*	128	6	1.138	-191.8	7.3	0.007
[8]	PR*-P2R*-PR2*-P2R2*	128	8	1.056	-196.9	2.3	0.082
[9]	PR*-P2	128	3	2.293	-108.8	90.4	0.000
[10]	PR*-P2R*-P2	128	5	1.521	-157.0	42.1	0.000
[11]	PR*-PR2*-P2	128	5	1.451	-163.1	36.1	0.000
[12]	PR*-PR2*-P2R*-P2	128	7	1.116	-192.1	7.1	0.007
[13]	PR*-P2R2*-P2	128	5	1.094	-199.2	0.0	0.259
[14]	PR*-P2R*-P2R2*-P2	128	7	1.069	-197.6	1.6	0.116
[15]	PR*-PR2*-P2R2*-P2	128	7	1.064	-198.2	1.0	0.160
[16]	PR*-P2R*-PR2*-P2R2*-P2	128	9	1.044	-196.0	3.2	0.053
[17]	PR*-R2	128	3	4.538	-21.4	177.7	0.000
[18]	PR*-P2R*-R2	128	5	1.643	-147.1	52.1	0.000
[19]	PR*-PR2*-R2	128	5	1.431	-164.8	34.3	0.000
[20]	PR*-PR2*-P2R*-R2	128	7	1.167	-186.4	12.8	0.000
[21]	PR*-P2R2*-R2	128	5	2.808	-78.5	120.7	0.000
[22]	PR*-P2R*-P2R2*-R2	128	7	2.785	-75.1	124.1	0.000

[23]	PR*-PR2*-P2R2*-R2	128	7	1.137	-189.7	9.5	0.002
[24]	PR*-P2R*-PR2*-P2R2*-R2	128	9	1.053	-194.9	4.3	0.030
[25]	PR*-P2-R2	128	4	1.488	-162.0	37.2	0.000
[26]	PR*-P2R*-P2-R2	128	6	1.247	-180.2	19.0	0.000
[27]	PR*-PR2*-P2-R2	128	6	1.235	-181.4	17.8	0.000
[28]	PR*-PR2*-P2R*-P2-R2	128	8	1.071	-195.1	4.1	0.034
[29]	PR*-P2R2*-P2-R2	128	6	1.289	-176.0	23.2	0.000
[30]	PR*-P2R*-P2R2*-P2-R2	128	8	1.949	-118.5	80.7	0.000
[31]	PR*-PR2*-P2R2*-P2-R2	128	8	1.779	-130.1	69.1	0.000
[32]	PR*-P2R*-PR2*-P2R2*-P2-R2	128	10	1.000	-199.1	0.1	0.248

DynaFit Script and Experimental Data - Model Discrimination #2

```
;_____

[task]

   data = equilibria
   task = fit
   model = PR*-P2R2*-P2 ?

[components]

   P, R

[mechanism]

   P + R <===> P.R              :      Kpr    dissoc
   P.R + P.R <===> P.R.P.R      :      Kprpr  dissoc
   P + P <===> P.P              :      Kpp    dissoc

[constants]

   Kpr = 0.1 ?
   Kprpr = 0.1 ?
   Kpp = 0.1 ?

[responses]

   P.R = 10 ?
   P.R.P.R = 10 ?

[concentrations]

[data]

    variable    P, R
    set          alldata

[output]

    directory   ./users/Miller_GP/070510/output/fit-002d

[settings]

{Marquardt}
   IterationsPerParameter = 300

;_____

[task]
```

```
    data = equilibria
    task = fit
    model = PR*-P2R2-P2 ?

[mechanism]

    P + R <===> P.R              :     Kpr    dissoc
    P.R + P.R <===> P.R.P.R      :     Kprpr  dissoc
    P + P <===> P.P              :     Kpp    dissoc

[constants]

    Kpr = 0.1 ?
    Kprpr = 0.1 ?
    Kpp = 0.1 ?

[responses]

    P.R = 10 ?

;_____

[task]

    data = equilibria
    task = fit
    model = PR*-P2R*-P2R2*-P2 ?

[mechanism]

    P + R <===> P.R              :     Kpr    dissoc
    P.R + P <===> P.P.R          :     Kppr   dissoc
    P.P.R + R <===> P.R.P.R      :     Kprpr  dissoc
    P + P <===> P.P              :     Kpp    dissoc

[constants]

    Kpr = 0.1 ?
    Kppr = 0.1 ?
    Kprpr = 0.1 ?
    Kpp = 0.1 ?

[responses]

    P.R = 10 ?
    P.P.R = 10 ?
    P.R.P.R = 10 ?

;_____

[task]

    data = equilibria
    task = fit
    model = PR*-P2R*-P2R2-P2 ?

[mechanism]
```

```
   P + R <===> P.R                :      Kpr    dissoc
   P.R + P <===> P.P.R            :       Kppr  dissoc
   P.P.R + R <===> P.R.P.R        :      Kprpr  dissoc
   P + P <===> P.P                :      Kpp    dissoc

[constants]

   Kpr = 0.1 ?
   Kppr = 0.1 ?
   Kprpr = 0.1 ?
   Kpp = 0.1 ?

[responses]

   P.R = 10 ?
   P.P.R = 10 ?

;_____

[task]

   data = equilibria
   task = fit
   model = PR*-P2R-P2R2*-P2 ?

[mechanism]

   P + R <===> P.R                :      Kpr    dissoc
   P.R + P <===> P.P.R            :       Kppr  dissoc
   P.P.R + R <===> P.R.P.R        :       Kprpr dissoc
   P + P <===> P.P                :      Kpp    dissoc

[constants]

   Kpr = 0.1 ?
   Kppr = 0.1 ?
   Kprpr = 0.1 ?
   Kpp = 0.1 ?

[responses]

   P.R = 10 ?
   P.R.P.R = 10 ?

;_____

[task]

   data = equilibria
   task = fit
   model = PR*-P2R-P2R2-P2 ?

[mechanism]

   P + R <===> P.R                :      Kpr    dissoc
   P.R + P <===> P.P.R            :       Kppr  dissoc
```

```
      P.P.R + R <===> P.R.P.R        :      Kprpr  dissoc
      P + P <===> P.P                :      Kpp    dissoc

[constants]

   Kpr = 0.1 ?
   Kppr = 0.1 ?
   Kprpr = 0.1 ?
   Kpp = 0.1 ?

[responses]

   P.R = 10 ?


;_____


[task]

   data = equilibria
   task = fit
   model = PR*-PR2*-P2R2*-P2 ?

[mechanism]

   P + R <===> P.R                :      Kpr    dissoc
   P.R + R <===> P.R.R            :      Kprr   dissoc
   P.R.R + P <===> P.R.P.R        :      Kprpr  dissoc
   P + P <===> P.P                :      Kpp    dissoc

[constants]

   Kpr = 0.1 ?
   Kprr = 0.1 ?
   Kprpr = 0.1 ?
   Kpp = 0.1 ?

[responses]

   P.R = 10 ?
   P.R.R = 10 ?
   P.R.P.R = 10 ?


;_____


[task]

   data = equilibria
   task = fit
   model = PR*-PR2*-P2R2-P2 ?

[mechanism]

   P + R <===> P.R                :      Kpr    dissoc
   P.R + R <===> P.R.R            :      Kprr   dissoc
   P.R.R + P <===> P.R.P.R        :      Kprpr  dissoc
   P + P <===> P.P                :      Kpp    dissoc
```

```
[constants]

   Kpr = 0.1 ?
   Kprr = 0.1 ?
   Kprpr = 0.1 ?
   Kpp = 0.1 ?

[responses]

   P.R = 10 ?
   P.R.R = 10 ?

;_____

[task]

   data = equilibria
   task = fit
   model = PR*-PR2-P2R2*-P2 ?

[mechanism]

   P + R <===> P.R                  :     Kpr    dissoc
   P.R + R <===> P.R.R              :     Kprr   dissoc
   P.R.R + P <===> P.R.P.R          :     Kprpr  dissoc
   P + P <===> P.P                  :     Kpp    dissoc

[constants]

   Kpr = 0.1 ?
   Kprr = 0.1 ?
   Kprpr = 0.1 ?
   Kpp = 0.1 ?

[responses]

   P.R = 10 ?
   P.R.P.R = 10 ?

;_____

[task]

   data = equilibria
   task = fit
   model = PR*-PR2-P2R2-P2 ?

[mechanism]

   P + R <===> P.R                  :     Kpr    dissoc
   P.R + R <===> P.R.R              :     Kprr   dissoc
   P.R.R + P <===> P.R.P.R          :     Kprpr  dissoc
   P + P <===> P.P                  :     Kpp    dissoc

[constants]

   Kpr = 0.1 ?
```

```
   Kprr  = 0.1 ?
   Kprpr = 0.1 ?
   Kpp   = 0.1 ?

[responses]

   P.R = 10 ?

;_____

[set:alldata]

...
... AS ABOVE IN MODEL DISCRIMINATION #1
...

[end]
```

Results - Model Discrimination #2

Minimum sum of squares = 0.185593

	model	nD	nP	SSrel	AICc	Δ AICc	weight
[1]	PR*-P2R2*-P2	128	5	1.029	-199.2	3.4	0.058
[2]	PR*-P2R2-P2	128	4	1.028	-201.5	1.1	0.183
[3]	PR*-P2R*-P2R2*-P2	128	7	1.004	-197.9	4.8	0.030
[4]	PR*-P2R*-P2R2-P2	128	6	1.003	-200.2	2.4	0.095
[5]	PR*-P2R-P2R2*-P2	128	6	1.003	-200.2	2.4	0.095
[6]	PR*-P2R-P2R2-P2	128	5	1.002	-202.6	0.0	0.318
[7]	PR*-PR2*-P2R2*-P2	128	7	1.001	-198.3	4.4	0.036
[8]	PR*-PR2*-P2R2-P2	128	6	1.000	-200.6	2.0	0.118
[9]	PR*-PR2-P2R2*-P2	128	6	1.043	-195.2	7.4	0.008
[10]	PR*-PR2-P2R2-P2	128	5	1.028	-199.3	3.3	0.061